

Broadband, high spectral resolution 2-D wavelength-parallel polarimeter for Dense WDM systems

S. X. Wang, Shijun Xiao, A. M. Weiner

School of Electrical & Computer Engineering, Purdue University, West Lafayette, IN 47907-1285, USA
wang7@ecn.purdue.edu, sxiao@ecn.purdue.edu, amw@ecn.purdue.edu

Abstract: A broadband wavelength-parallel polarimeter has been designed for polarization measurements of multiple Dense WDM channels in parallel, which is based on a 2-D spectral disperser via a diffraction grating and a virtually-imaged phased-array (VIPA). At a hyperfine 2.8 GHz sub-channel spacing, we have demonstrated spectral polarization measurements of ~1500 sub-channels (~32 nm spectral range), with a potential total measurement time of less than 5 ms.

©2005 Optical Society of America

OCIS codes: (120.5410) Polarimetry; (060.2330) Fiber optics communications; (060.2370) Fiber optic sensors.

References and links

1. M. Boroditsky, K. Cornick, C. Antonelli, M. Brodsky, S.D. Dods, N.J. Frigo, P. Magill, "Comparison of System Penalties from First- and Multiorder Polarization-Mode Dispersion," *IEEE Photonics Technol. Lett.* **17**, 1650-1652, 2005.
2. S. M. Reza Motaghian Nezam, J. E. McGeehan, A. E. Willner, "Degree-of-Polarization-Based PMD Monitoring for Subcarrier Multiplexed Signals Via Equalized Carrier/Sideband Filtering," *J. Lightwave Technol.* **22**, 1078-1085, 2004.
3. M. Boroditsky, M. Brodsky, N.J. Frigo, "In-Service Measurements of Polarization-Mode Dispersion and Correlation to Bit-Error Rate," *IEEE Photonics Technol. Lett.* **15**, 572-574, 2003.
4. P. B. Phua, J. M. Fini, H. A. Haus, "Real-Time First and Second order PMD Characterization Using Averaged State-of-Polarization of filtered Signal and Polarization Scrambling," *J. Lightwave Technol.* **21**, 982-989, 2003.
5. J. C. Rasmussen, "Automatic PMD and Chromatic Dispersion Compensation in High Capacity Transmission," Session TuB3.4, LEOS Summer Topical Meetings, 2003
6. M. Boroditsky, M. Brodsky, N.J. Frigo, P. Magill, J. Evankow, "Viewing Polarization 'Strings' on Working Channels: High-Resolution Heterodyne Polarimetry," Session We1.4.5, European Conference on Optical Communication, 2004.
7. P.M Krummrich, E.D. Schmidt, "Field Trial Results on Statistics of Fast Polarization Changes in Long Haul WDM Transmission Systems," Session OThT6, Optical Fiber Communications Conference, 2005
8. S. X. Wang, A. M. Weiner, "Fast wavelength-parallel polarimeter for broadband optical networks," *Opt. Lett.* **29**, 923-925, 2004.
9. M. Bass, E. W. Van Stryland *Handbook of Optics VII* (McGraw-Hill, 1994), Chap. 22.
10. S. Xiao, A. M. Weiner, "2-D wavelength demultiplexer with potential for ≥ 1000 channels in the C-band," *Opt. Express* **12**, 2895-2902, 2004. <http://www.opticsexpress.org/abstract.cfm?URI=OPEX-12-13-2895>.
11. M. Shirasaki, "Large Angular Dispersion by a Virtually Imaged Phased Array and Its Application to a Wavelength Demultiplexer," *Opt. Lett.* **21**, 366-368, 1996.

1. Introduction

High resolution and high speed polarization sensing is critical in WDM and Dense WDM applications such as state of polarization (SOP) measurement, polarization mode dispersion (PMD) monitoring for real time PMD compensation, and estimating PMD induced system penalties [1]. Some of the common PMD monitoring methods proposed recently either make

use of the Degree of Polarization (DOP) [2] or the wavelength dependent SOP [3,4]. Wavelength-dependent SOP can, in principle, provide greater information than DOP alone but it requires measurements at multiple wavelengths. Current commercial polarization sensing products are mostly single channeled devices. It is possible to perform multiple channel SOP measurements by using a single-channel polarization analyzer for each optical channel [5], but cost and package size increase proportionally with the number of channels, and can become impractical. This problem is often overcome by using a tunable filter or tunable laser to sweep through individual channels one at a time [3,4,6]; however, this method can increase measurement time substantially due to the tuning and settling time of the filter. Since SOP within a fiber can occasionally vary on a millisecond time scale or less [7], faster monitoring methods are needed, especially for use in near-real-time adaptive PMD compensation applications. Here, for the first time to our knowledge, we present a novel polarimeter design able to capture polarization states of ~1500 sub-channels at 2.8GHz sub-channel spacing, with potential total measurement time of less than 5ms. Such an apparatus could allow the sensing of SOP variation within individual DWDM channels with 2.8 GHz resolution in parallel with no moving parts.

2. Experimental setup

The high spectral resolution polarization sensor is composed of two main stages. Shown in Fig. 1, the first stage is a polarization component selector, which consists of a pair of fast switching ferroelectric liquid crystal (FLC) retarders and a polarizer. The FLCs (from Displaytech) were anti-reflection coated, and were designed to have fixed quarter-wave phase retardation for 1550nm light. The fast optic axis of the first FLC switched between 90° and 135° , the axis of the second FLC switched between 135° and 180° (0°), and the polarizer was fixed at horizontal (0°). The FLC pair and the polarizer were used to sequentially transform the SOP permitting determination of four polarization components of the light under test [8]. Ideally, the four measurement steps analyze right hand circular, linear 0° , 45° , and 90° , polarization components respectively. Each polarization alteration takes less than 0.1ms. With the knowledge of these four polarization components, the polarization Stokes Parameters of the light can be found [9]. In the second stage of the polarization sensor, the light is spectrally dispersed onto an InGaAs detector array for wavelength-parallel operation. In previous work, we used a diffraction grating for one-dimensional (1-D) spectral dispersion, along with a line scan camera allowing measurements of 256 spectral components over a ~100 nm band in parallel in under 1 ms [8]. In order to attain higher spectral resolution over a broad bandwidth, we adopted a 2-D spectral dispersion geometry [10] via a virtually imaged phased array (VIPA) [11] and a diffraction grating.

Figure 2(a) shows our high resolution 2-D spectral disperser and wavelength-parallel measurement setup. An amplified spontaneous emission (ASE) source with a 3dB bandwidth of 38 nm centered at 1548nm was used for the experiment. The ~2mm beam was first focused into a VIPA (provided by Avanex) by a cylindrical lens ($f=180\text{mm}$). The VIPA was designed with a free spectral range (FSR) of 50GHz (0.4nm), periodically dispersing segments of 50GHz of bandwidth in the x-direction. It was tilted roughly 3° in the z-direction, resulting in $\sim 2.15^\circ/\text{nm}$ of angular dispersion. An 1100 lines/mm grating was placed subsequently to spatially separate all the FSRs of the VIPA in the y direction. The incident beam was $\sim 71.4^\circ$ with respect to the normal of the grating surface to yield $0.097^\circ/\text{nm}$ angular

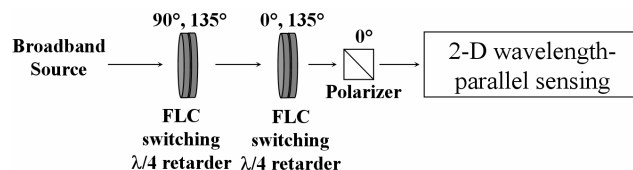


Fig. 1. Broadband high resolution spectral polarimeter setup.

dispersion. In order to attain better FSR isolations, a $2.5\times$ y-axis beam expander was added before the grating to increase the beam width at the grating to $\sim 5\text{mm}$ to result in higher spectral resolution in the grating dispersion direction. Figure 2(b) shows a schematic view of the spatial pattern of the 2-D dispersion at the image plane of the focusing lens after the grating. Finally, the resultant 2-D spectrally dispersed beam was focused onto a 2-D InGaAs camera (Indigo Alpha NIR™) with 320×256 pixels, and $30\times 30\ \mu\text{m}^2$ pixel size. The camera was tilted $\sim 2.5^\circ$ to line up the pixel columns with the FSRs. As shown in Fig. 2(c), the camera aperture contained 82 total FSRs, covering a wavelength range of 32.8nm from 1536.1nm to 1568.9nm of the ASE source. A continuous wave (CW) laser source with

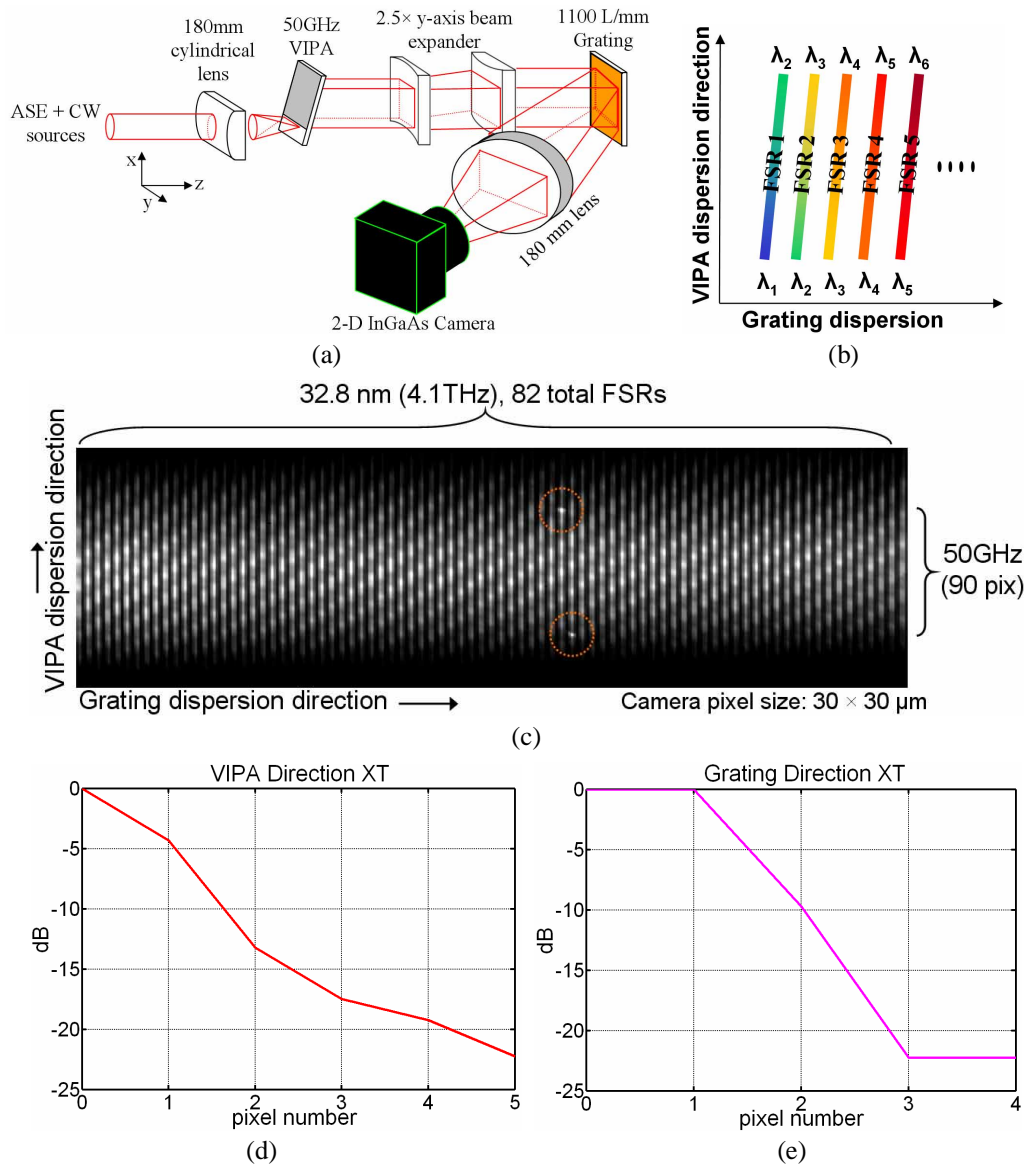


Fig. 2. (a) Setup of the 2-D wavelength-parallel sensing. (b) Schematic spatial arrangements of the 2-D dispersed spectrum. (c) Camera capture showing spatially resolved FSRs and the covered spectral range of the ASE source. The two circled dots indicate two different orders of diffraction. (d) VIPA direction cross-talk (XT) measurement of neighboring pixels with a single CW laser source centered at reference pixel labeled 0. (e) FSR cross-talk measurement for a single CW laser source positioned on the FSR centered between reference pixels labeled 0 and 1.

~0.1pm bandwidth was coupled together with the ASE input. The CW source experienced multiple orders of diffraction from the VIPA, but only two of the strongest ones were visible on the camera, and they showed up as white dots on two neighboring FSRs (circled in Fig. 2(c)). The two orders of diffraction of the CW source were used as FSR-cutoff indicators; they marked the 50 GHz range (90 pixels) of the FSR in the VIPA dispersion direction. With the ASE source turned off, the CW source was used for determining sub-channel isolation. Not to be confused with a DWDM channel, we use “sub-channel” from here on to represent a small bandwidth segment within a DWDM channel. In Fig. 2(d), pixel #0 was taken as the center of the CW source spot on the camera, the light intensity drops to -22.25 dB at pixel #5. In a case of high wavelength-dependent SOP spreading where crosstalk is a main concern, one out of every 5 or more pixels should be used as a sub-channel to achieve better than -20dB isolation between neighboring sub-channels in the VIPA dispersion direction. However, in our experiments described below, wavelength-dependent SOP spreading was mild (owing to the high spectral resolution), we averaged together the readings from each group of 5 pixels in the VIPA dispersion directions to represent one wavelength sub-channel to achieve better signal to noise ratio, while covering 2.8GHz of bandwidth (or 0.0224nm) per sub-channel. Narrower sub-channel spacing could be implemented at the cost of higher sub-channel cross-talk, and vice versa. The 2.8 GHz sub-channel division allowed 1476 total sub-channels within the aperture of the camera, and essentially spans the entire light-wave communications C-band. In the grating dispersion direction, the neighboring FSRs were spaced by 4 camera pixels apart, and the cross-talk between FSRs was less than -22.3 dB as shown in Fig. 2(e).

3. Experimental results

The wavelength-parallel polarimeter design based on the 2-D spectral dispersion should be able to measure wavelength dependent SOP within each DWDM channel for multiple channels in parallel. We have performed experiments that demonstrated wavelength-dependent SOP ($SOP_{(\lambda)}$) measurements using the 2-D dispersion setup. The source used was a mode-locked laser with ~0.5mW total power, centered at 1580nm, and has a 3dB bandwidth of ~62nm. The 2-D dispersion setup covered 32.8nm of the laser spectrum from 1536.1nm to 1568.9nm, with 2.8GHz resolution. First test was performed by launching the polarized

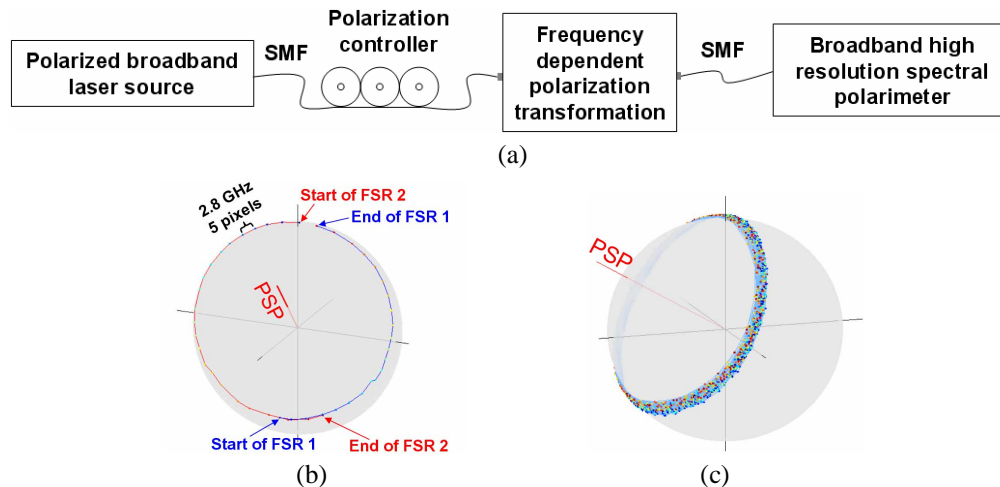


Fig. 3. (a) Experimental setup diagram for producing and measuring wavelength dependent SOP over a broad wavelength span. (b) Measured SOP data of 2 neighboring FSRs of the VIPA output, equivalently 100GHz spectral range. (c) Measured SOP data of all 82 FSRs. Note: the reason the PSP axis of the PM fiber is not aligned with linear polarization is because the PSP has been shifted by the single mode fiber (SMF) after the PM fiber.

broadband source into a frequency dependent polarization transformer consisting of a strand of approximately 7.5m long polarization maintaining (PM) fiber, which acted as a 1st order PMD emulator. This piece of PM fiber had a beat-length of $\sim 4\text{mm}$ ($\Delta n \approx 3.88 \times 10^{-4}$) at $\lambda = 1550\text{nm}$, and provided approximately a half-wave of phase retardation difference between f and $f + 50\text{GHz}$, where f is the frequency of an arbitrary frequency component near $\lambda = 1550\text{nm}$. The half-wave retardation difference should allow the $\text{SOP}_{(\lambda)}$ corresponding to a 50GHz frequency range to spread out in a circular fashion half way around the Poincarè sphere, centered at the principle state of polarization (PSP) axis of the PM fiber. To see the continuity of neighboring FSRs, two adjacent FSRs totaling a range of 100GHz were plotted in Fig. 3(a) respectively in red and blue. As shown in the illustration, each 50GHz looped roughly half way around the sphere, and the two FSRs of $\text{SOP}_{(\lambda)}$ connected perfectly with 2.8GHz separation (see Fig. 3(b)), making approximately a full circle around the sphere, centered at the PSP of the PM fiber. When all 32.8nm range of $\text{SOP}_{(\lambda)}$ were plotted on the Sphere, the resultant trace looped roughly 41 times around the same circle (see Fig. 3(c)), which was in accord with expectation.

We also tried to perform measurements of more complicated $\text{SOP}_{(\lambda)}$ patterns covering the entire Poincarè Sphere by replacing the 7.5m PM fiber with more complex frequency dependent polarization transformers. The first polarization transformer was a concatenation of eight pieces of PM fibers with their optic axes randomly oriented from one another. The eight segments of PM fibers had different individual lengths and had a total length of 6.12m. The second polarization transformer also consisted of eight segments of PM fiber but with a total length of 3.48m. When only the 6.12m polarization transformer was used, the produced wavelength-spread SOP showed a closely spaced $\text{SOP}_{(\lambda)}$ pattern (see Fig. 4(a)). When the single piece of 7.5m long PM fiber used in the first test was connected subsequently to the 6.12m polarization transformer, the output $\text{SOP}_{(\lambda)}$ spread out more rapidly and covered most of the sphere as shown in Fig. 4(b). While a typical single-channel polarimeter would see only a depolarized light, the broadband high resolution spectral polarimeter was able to unveil the details of the spectrally dependent SOP information. Finally, all three polarization transformers were connected together in the sequence—the 6.12m 8-segment PM fiber, the 3.48m 8-segment PM fiber, and the 7.5m single PM fiber. At a particular input SOP, the combined polarization transformers were able to generate an extreme case of frequency dependent polarization scrambling. The output $\text{SOP}_{(\lambda)}$ in this case completely covered the Poincarè Sphere (see Fig. 4(c)), showing that the polarimeter was able to measure all polarization states around the Sphere.

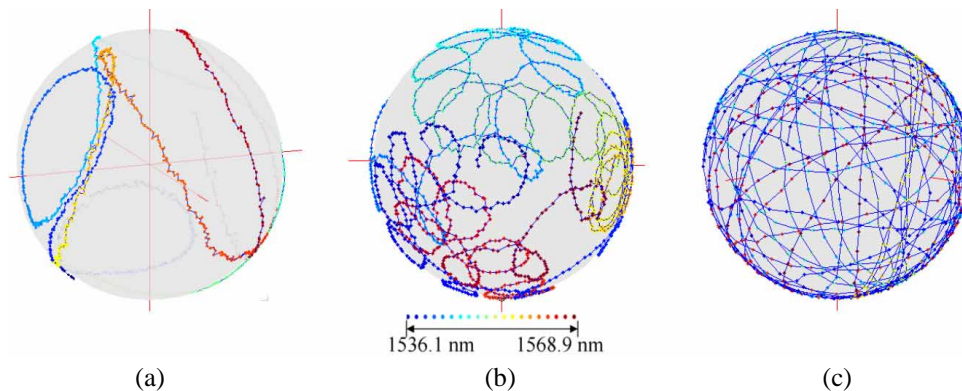


Fig. 4. (a) Output $\text{SOP}_{(\lambda)}$ produced by a 6.12m long 8-segment PM fiber. (b) Output $\text{SOP}_{(\lambda)}$ of the 8-segment PM fiber connected with a single-piece 7.5m PM fiber. (c) Output $\text{SOP}_{(\lambda)}$ of two different 8-segment PM fibers with the single piece 7.5m PM fiber.

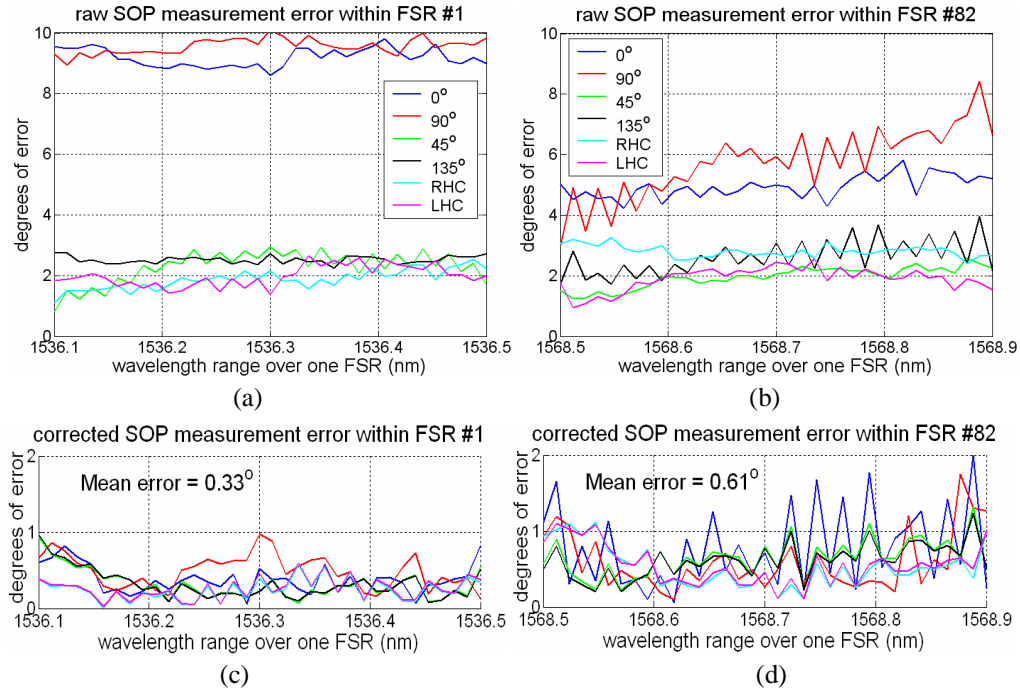


Fig. 5. SOP measurement error of 6 different known SOP points around the Poincaré Sphere over measured wavelength ranges. (a) SOP error from 1536.1 nm to 1536.5 nm and (b) SOP error from 1568.5 nm to 1568.9 nm before software correction. (c) Corrected SOP error from 1536.1 nm to 1536.5 nm and (d) corrected SOP error from 1568.5 nm to 1568.9 nm.

Due to wavelength dependent retardance of FLCs and non-ideal FLC switching behavior (i.e., switching angle slightly different than the 45° design value), a software correction was applied to the measurement results to improve measurement accuracy. The reader is directed to [8] for correction algorithm and error representation details. To evaluate the measurement accuracy of the polarimeter, we measured six known polarizations around the Poincaré Sphere produced by a Polarcor™ polarizer and a broadband quarter wave plate. The six known polarizations produced were 0° , 45° , 90° , 135° , right hand circular (RHC), and LHC. The measured SOP showed a worst case error of up to 16° and 10° on the Poincaré sphere respectively before and after the correction procedure for worst case polarization states, which we believe was due to a slight nonlinearity of the 2-D camera response. In principle, camera nonlinearity can be corrected in software. However, for the current paper we chose a different but analogous approach. We replaced the 2-D camera with the more linear 1-D detector array (Sensors Unlimited SU256LX1.7T1™) which we used in our previous work [8], with the array aligned in the VIPA dispersion direction. The 1-D detector array aperture was masked with a $50\mu\text{m}$ slit running parallel to the array direction and mounted on a translation stage. The slit was used so that only one FSR was allowed to be measured at a time, and the translation stage enabled the 1-D detector array to shift to different spatial positions for selecting different FSRs. Measurements were taken at two FSRs approximately 32.8nm wavelengths apart, corresponding to the 82 FSR range covered by the 2-D camera setup from earlier. 0° and 90° linear polarization measurements exhibited the worst cases of SOP measurement, up to 10° of error at some wavelengths before software correction as shown in Fig. 5(a, b). After correction, the worst case SOP error for any polarization was observed to be less than 2° (see Fig. 5(c, d)). The mean error was only 0.33° and 0.61° for FSRs #1 and #82, respectively. Our results demonstrate that our 2-D optical configuration is compatible with high accuracy polarization measurements, similar to that obtained in our previous 1-D

polarimetry experiments [8]. In our previous design [8], a 1-D camera (Sensors Unlimited SU256LX1.7T1) with readout time of 0.0528ms was used for data acquisition. Adding to the 0.1ms FLC switching time, we predicted the measurement speed for a set of 4 polarization components to be less than 1ms $((0.0528+0.1)\text{ms}\times 4)$, which yielded one complete SOP measurement set. In a verification experiment, we used a function generator as the trigger source for the polarimeter setup, and achieved measurement time of 0.8ms for one complete set of raw SOP measurement data. Software correction time was not measured because it depends on the processing speed and efficiency of coding, which can also be improved with a dedicated chip. In the current 2-D spectral dispersion setup, the measurement time was limited by the 30 frames/sec frame rate of the 2-D camera. The measurement speed could be much improved by employing a fast 2-D camera such as the Sensors Unlimited SU320MSW, which has the capability of running at 1000 frames/sec. Using the same time budget calculation as the 1-D setup, we estimate a potential total measurement time to be less than 5 ms for the 2-D spectral polarimeter.

4. Conclusion

We have demonstrated a broadband, high spectral resolution 2-D wavelength-parallel polarimeter capable of performing 2.8 GHz-spaced sub-channel polarization measurement for Dense WDM channels in parallel. Our experimental configuration consisted of close to 1500 sub-channels, spanning 32.8 nm, essentially covering the entire of the light-wave communications C-Band. Measurement accuracy was deteriorated due to the nonlinear response of our 2-D InGaAs camera; however, it was shown that with a more linear 2-D detector array, measurement accuracy can potentially be kept to within 2° on the Poincaré Sphere for any polarization state and at any wavelength. A projected measurement time of $<5\text{ms}$ for an entire set of SOP data should be achievable with a fast 2-D camera, which would allow this spectral polarimeter for use in many near-real-time optical network monitoring applications.

We gratefully acknowledge many helpful discussions with Peter Miller of CRI Inc., and the donation of the VIPA from Chris Lin of Avanex Corporation. This work was supported by NSF grant numbers 0140682-ECS and 0501366-ECS.